Controlled Sol-gel Transitions by Actuating Molecular Machine based Supramolecular Polymers

Antoine Goujon,[a] Giacomo Mariani,[b] Thomas Lang,[a] Emilie Moulin,[a] Michel Rawiso,[a] Eric Buhler,[b] and Nicolas Giuseppone[a]*

[a] SAMS research group – University of Strasbourg – Institut Charles Sadron, CNRS – 23 rue du Loess, BP 84047, 67034 Strasbourg Cedex 2, France

[b] Matière et Systèmes Complexes (MSC) Laboratory, UMR CNRS 7057, Sorbonne Paris Cité, University of Paris Diderot-Paris VII, Bâtiment Condorcet, 75205 Paris Cedex 13, France

ABSTRACT: The implementation of artificial molecular machines in polymer science is an important objective that challenges chemists and physicists in order to access an entirely new class of smart materials. To design such systems, the amplification of a mechanical actuation from the nanoscale up to a macroscopic response in the bulk material is a central issue. In this article we show that bistable [*c*2]daisy chain rotaxanes (*i.e.* molecular muscles) can be linked into main-chain Upy-based supramolecular polymers. We then reveal by an in depth quantitative study that the pH actuation of the mechanically active rotaxane at the nanoscale influences the physical reticulation of the polymer chains by changing the supramolecular behavior of the Upy units. This nano-actuation within the local structure of the main chain polymer results in a mechanically controlled sol-gel transition at the macroscopic level.

Introduction

Molecular machines have become a subject of major interest during the past fifty years because they can make use of mechanical work at nanoscale in order to produce new functions by energy transduction.[1–4] In cells, biomolecular machines participate for instance in the copy of the genetic code, in various processes of transport, and in the synthesis of ATP.[5,6] When working together in an integrated system, such machines can also amplify their motion up to the macroscopic scale. This is particularly striking when looking at muscles: their macroscopic motion originates from a hierarchical dynamics spanning all over the length scales from myosin heads to sarcomeric units, then myofibrils, and finally muscular fibers.[7] After intense investigations towards the design of artificial molecular machines as individual units, chemists are currently realizing that such an amplification of nanoscale motions can be of first interest for material science.[3,8–10] Indeed, artificial materials integrating nanomachines should be able to behave as autonomous actuators, *i.e.* with nano-mechanical units embedded in the bulk of the material itself. Ultimately, they promise to give access to mechanically active materials and actuators working out-of-equilibrium when fueled by an external source of energy.[11–13] Toward this goal, one of the first aspects to investigate relates to the various possible ways for linking molecular machines together in order to amplify their dynamic properties at the level of the entire systems. For instance, recent efforts have been directed towards the integration of individual "molecular muscles" (*i.e.* [*c*2]daisy chain rotaxanes[14,15]) introduced by Sauvage[16] within main chain polymers. Stoddart[17] and Grubbs[18] independently reported in 2009 the synthesis of short covalent oligomers made of [*c*2]daisy chain rotaxanes. More recently, our group reported the integration of thousands of molecular machines up to the microscopic scale using bistable rotaxane-based molecular machines coordinated within single chain metallo-supramolecular polymers.[19] Similar [*c*2]daisy chain rotaxanes were then linked into bundles of fibers,[20,21] demonstrating mechanical actuation of their morphologies at mesoscale.

Hereafter we describe a new step in the integration of bistable [*c*2]daisy chain rotaxanes at higher length scales by showing the mechanically-triggered macroscopic sol-gel transition of a hydrogen-bonded supramolecular polymer.

Results and discussion

Among the collection of hydrogen-bonding recognition patterns available,[22,23] the 2-Ureido-4[1H]-pyrimidinone (Upy)[24] has been shown to dimerize in solution with very high association constants (K_{dim} = 5.7 x 10^7 M^{-1} in chloroform and 5.9 x 10^8 M^{-1} in toluene).[25] The unit was extensively used to access various assemblies, going from discrete architectures[26] to supramolecular polymers and soft materials showing interesting structural and mechanical properties.[27–29] More particularly, a few examples of supramolecular polymers based on Upy-functionalized rotaxanes have been reported.[30,31] However, these rotaxanes did not show bistability and, as a consequence, their potential as actuators or as dynamic materials was not studied.

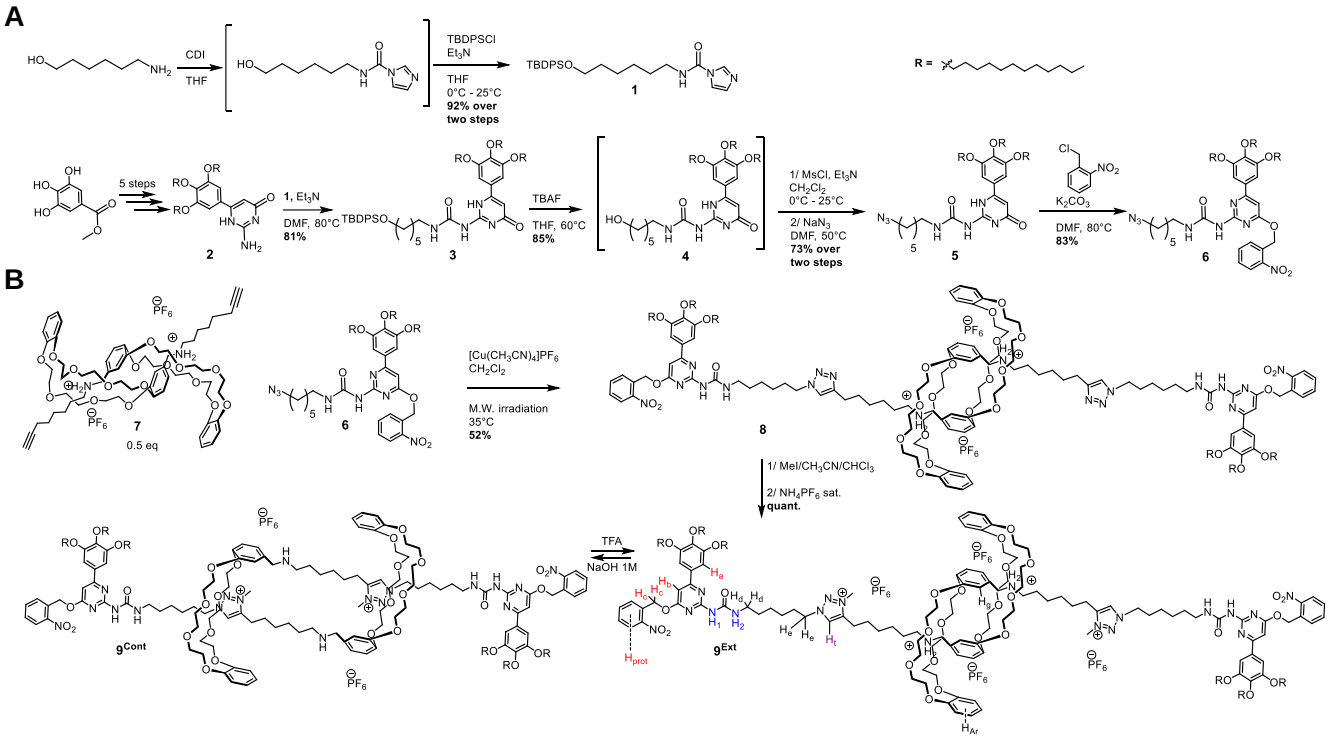

Scheme 1. (**A**) Synthetic route towards azide **6**. (**B**) Synthetic route towards extended $\mathbf{9}^{\mathbf{Ext}}$ and contracted $\mathbf{9}^{\mathbf{Cont}}$ rotaxanes.

Considering the interest of the high binding constant of Upy fragments for growing high molecular weight bistable [*c*2]daisy chain supramolecular polymers in solution, we established the synthetic route described in Scheme 1. The use of a tris-C12 gallic acid moiety attached to the Upy was envisioned to ensure solubility in organic solvents and to enforce lateral aggregation of polymer chains by Van-der-Waals and π-π-stacking interactions.[32] The hydrogen bonding pattern of the Upy was also protected using the photo-labile 2-nitrobenzyl group in order *i*) to simplify the synthesis and purification of **8**, and *ii*) to ensure that the supramolecular polymerization can be triggered only when necessary. Indeed, it is known that, upon irradiation at 365 nm, uncaging of the UPy group triggers the formation of Upy-Upy dimers via hydrogen bonding association.[31,33]

First, isocytosine **2** was prepared according to the literature[32] by heating at reflux the corresponding ethyl malonate precursor in ethanol with guanidinium carbonate. In parallel, 6-amino-1-hexanol was treated with carbonyldiimidazole (CDI), and then with TBDPSCl in basic conditions to furnish compound **1** with a very good yield (Scheme 1a). Isocytosine **2** and compound **1** were coupled in DMF at 80°C to give Upy derivative **3**. After deprotection using a 1M TBAF solution in THF, alcohol **4** was activated using methanesulfonyl chloride and then treated with sodium azide to produce azide **5**. The 2-nitrobenzyl photolabile group was finally introduced to yield compound **6**, which was further engaged in a copper-catalyzed 1,3 dipolar cycloaddition reaction with **7** under microwave irradiation, yielding Upy-functionalized [c2]daisy chains **8** with a yield of 52% (Scheme 1b). Note that pseudorotaxane **7** was prepared in nine steps following known procedures from the literature.[34] The final step was carried out in a mixture of methyl iodide, acetonitrile and chloroform to selectively methylate the triazole units of [c2]daisy chain **8** leading to the formation of extended triazolium rotaxane $\mathbf{9}^{\mathbf{Ext}}$. $\mathbf{9}^{\mathbf{Ext}}$ was converted into $\mathbf{9}^{\mathbf{Cont}}$ by deprotonation with a 1M sodium hydroxyde solution. In its extended form, the electron rich crown-ether of the [*c*2]daisy chain rotaxane complexes the electron poor secondary ammonium. After deprotonation of the amine, the ring glides toward the next electron poor group, which is the triazolium, leading to a reduction of the size of the molecule, and as monitored by ^{1}H NMR (Figure 1).

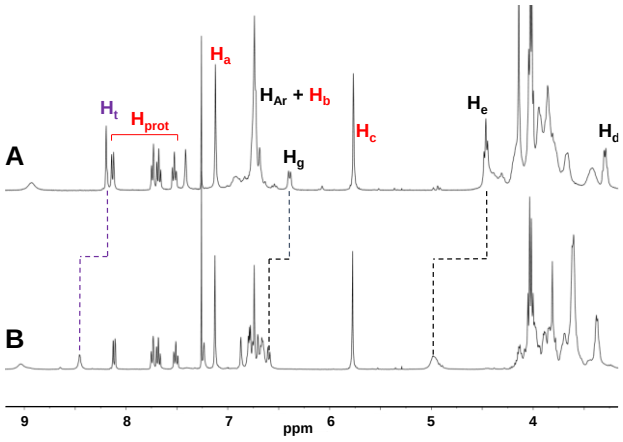

Figure 1. ^{1}H NMR spectra showing the actuation between extended $\mathbf{9}^{\mathbf{Ext}}$ (**A**) and contracted $\mathbf{9}^{\mathbf{Cont}}$ (**B**) rotaxanes. The labelling of the proton resonance signals corresponds to the numbering of the protons used for the chemical structure of $\mathbf{9}^{\mathbf{Ext}}$ drawn in Scheme 1.

The triazolium proton H_t, initialy at δ = 8.20 in $\mathbf{9}^{Ext}$ shifts downfield to δ = 8.45 in $\mathbf{9}^{Cont}$. Other protons close to the triazolium group are also affected, especially H_e, and a splitting of the aromatic protons of the macrocycle (H_{ar}) is observed in the contracted form.

Compounds $\mathbf{9}^{Ext}$ and $\mathbf{9}^{Cont}$ were subsequently used as building blocks for the formation of supramolecular polymers. Experimentally, a 18 wt% solution of $\mathbf{9}^{Ext}$ in toluene (or xylene, see Table S1) was exposed to UV light using a 150W Xenon-Mercury lamp with a 320-375 nm filter. After 4 hours of irradiation, the solution turned to a dark-orange physical gel made of $\mathbf{10}^{Ext}$ (Figure 2). We determined a sol-gel transition temperature of 40°C for $\mathbf{10}^{Ext\text{-}S}$ at a concentration of 18 wt% in toluene. A sample of $\mathbf{10}^{Ext}$ gel was then dried under vacuum overnight and taken back in $CDCl_3$ for ^{1}H NMR analysis (Figure S1). All peaks related to the protecting group (H_{Prot} and H_c) disappeared while a drastic shift of the urea peaks H_1 and H_2, the appearance of H_3, and the broadening of all the other resonance signals were in agreement with the formation of a H-bonded supramolecular polymer formed in chloroform by Upy-Upy dimerization.[24] Even though the monomer could not be observed by ^{1}H NMR for this specific reason, the formation of the individual molecule $\mathbf{10}^{Ext}$ was confirmed by HRMS (ESI+) (Figure S2). As expected, a similar sol-gel transition was observed for the conversion of non-methylated rotaxane $\mathbf{8}^{Ext}$ after deprotection of the Upy units (Figures S3 and S4). However, surprisingly, UV irradiation of rotaxane $\mathbf{9}^{Cont}$ provided the corresponding deprotected compound as a solution ($\mathbf{10}^{Cont}$) (Figures S5 and S6).

Gel $\mathbf{10}^{Ext}$ was then treated with 2 equiv. of triethylamine (NEt_3) in order to investigate the effect of the contraction of the [c2]daisy chains on the structure of the gel. The gel instantly turned into a solution. Interestingly, the addition of 2 equiv. of hydrochloric acid (2M in Et_2O) yielded back the initial gel (Figure 2). However, upon addition of a base to the gel made of UV-deprotected **8**, we did not observe any phase transition (Figure S7). This observation can be explained by the lack of bistability without a well-defined triazolium station for the macrocycle, precluding any efficient contracted conformation for the deprotonated [c2]daisy chain **8**. In addition, this important control experiment excludes a gel-sol transition that would be the result of a deprotonation of the Upy unit. In the same direction, ^{1}H NMR spectra of **3** in $CDCl_3$ in presence of a large excess of triethylamine did not show any perturbation of the hydrogen-bonding unit (Figure S8). We can thus assume that the phase transition is directly related to the contraction and extension of the bistable [c2]daisy chains in the polymer network.

FTIR spectroscopy experiments were performed on $\mathbf{10}^{Ext}$ as a 18 wt% gel in toluene (50 mM), and $\mathbf{10}^{Cont}$ as a 16.6 wt% solution in toluene (50 mM) (Figure S9). The IR spectrum of $\mathbf{10}^{Ext}$ displayed N-H stretching bands at 3172 and 3070 cm^{-1}, and C=O stretching bands at 1692 and 1648 cm^{-1}. For $\mathbf{10}^{Cont}$, the spectrum displayed N-H stretching bands at 3174 and 3071 cm^{-1} and C=O stretching bands at 1687 and 1661 cm^{-1}. These similar stretching band values and the absence of free N-H band in the 3600-3500 cm^{-1} range confirmed the presence of hydrogen bonded Upy dimers in both supramolecular polymers, which are in agreement with the one reported in the literature.[35,36]

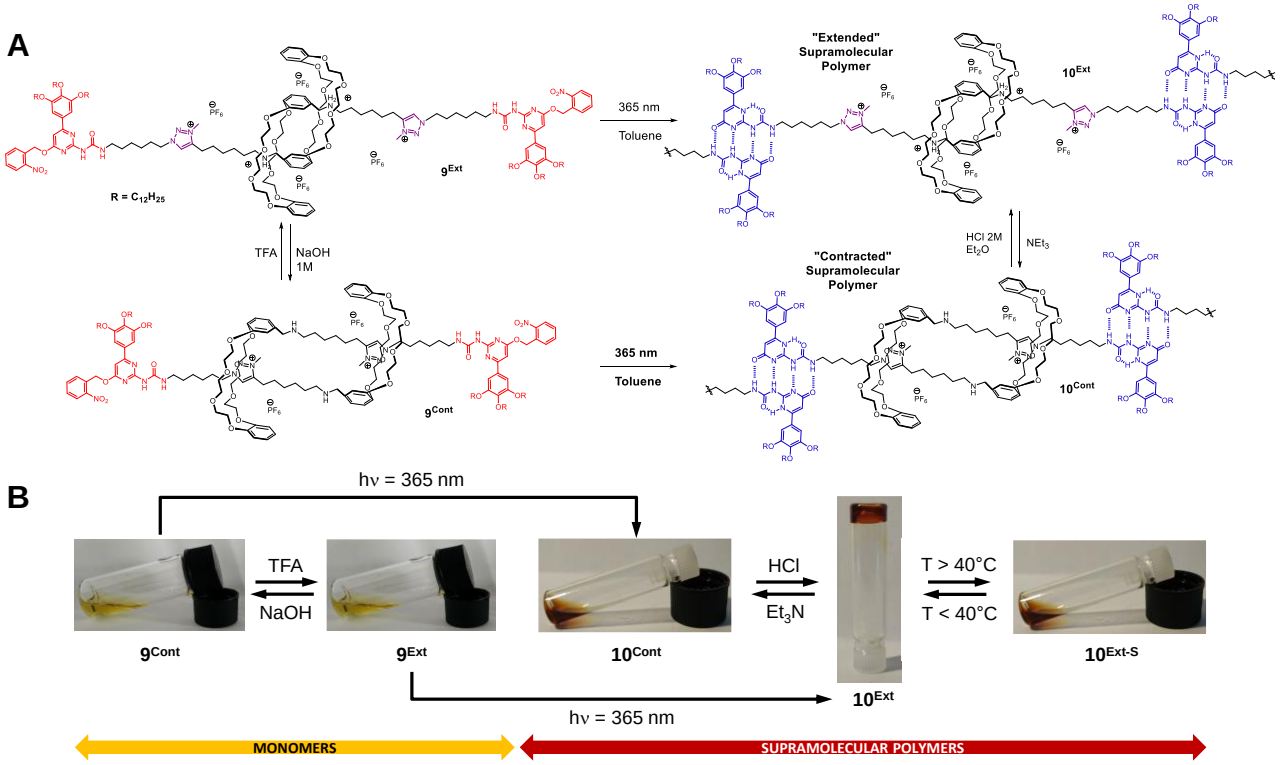

Figure 2. (**A**) Chemical structures of the molecules involved in the sol-gel system upon light-deprotection / supramolecular polymerization, and upon contraction / extension. (**B**) Physical states in toluene of the system represented in (**A**).

We then studied the binding constant of the Upy unit for **10**^{Cont} by Isothermal Titration Calorimetry (ITC).[37] 20 aliquots (5 µL each) of a 1 wt% solution of **10**^{Cont} in toluene (2.66 mM) were added into pure toluene, resulting in the enthalpogram displayed in Figures 3a and S10. By fitting the data with a dimer model, we measured an association constant K_a = 1.1 x 10^4 M^{-1}, and a positive enthalpy of dissociation ΔH_d = 2.5 x 10^1 kJ/mol, (*i.e.* ΔH_a negative). This exothermic character of the association process is in agreement with the formation of hydrogen bonds, but the association constant appears 4 orders of magnitude lower than classical Upy dimerization in toluene.[25] Differential Scanning Calorimetry (DSC) was also performed on both the gel made of **10**^{Ext} and the solution made of **10**^{Cont}. In the case of **10**^{Ext}, upon heating from 10 °C to 80 °C, two transitions were recorded at 39.6 °C and 74.9 °C. A hysteresis was observed while cooling down the sample, with transitions at 65.5 °C and 35.1 °C (Figure 3b). The transition at low temperature is explained by the melting point of the gel as already observed macroscopically at around 40°C. The second transition at 65.5 °C is attributed to the loss of the inter-chains organization, and not to Upy dimers dissociation or degradation which is expected to occur only above 227 °C.[36] Thermogravimetric Analysis (TGA) confirmed that these transitions were not related to the degradation of the compound as no event other than the evaporation of toluene was observed upon heating the gel sample **10**^{Ext} from 25 °C to 290 °C (Figure S11). Conversely, the DSC experiment performed on the solution of **10**^{Cont} did not show any signal in the 10 °C – 80 °C range, indicating the lack of organization beyond the main chain polymer.

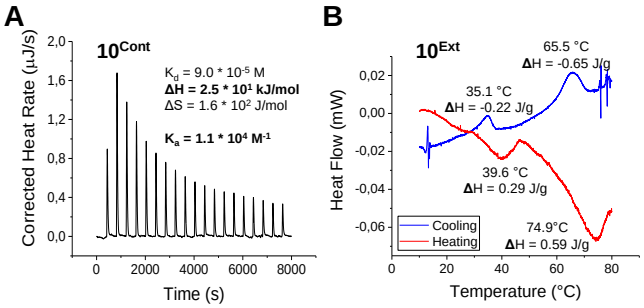

Figure 3. (**A**) ITC enthalpogram of contracted supramolecular polymer in toluene. (**B**) DSC signal of extended supramolecular polymer in toluene.

By combining these results with precedents from the literature, a first assumption can be made regarding the different physical states observed for **10**^{Ext} and **10**^{Cont} at room temperature. The stacking of ureido-triazine dimers[38,39] or of Upy-Upy dimers into helical column has been previously reported and well-studied.[32] Solvophobic interactions are believed to be responsible for the formation of these stacks because Upy-Upy dimers are flat and rigid discs, much more polar than the periphery made of C_{12}-functionnalized gallic acid which shields the stacks from the solvent. The formation of hydrogen bonds tends also to reinforce the aromatic character of the Upy delocalized system, increasing its ability to interact *via* π-stacking.[40] Moreover, in an apolar solvent such as toluene, the presence of the C_{12}-functionnalized gallic acid moieties reinforce the formation of the Upy stacks by additional π-stacking and Van-der-Waals interactions. It is thus reasonable to expect that the presence of these stacked structures beyond the main chain supramolecular polymers would create physical reticulating nodes,[41] leading to a three-dimensional network for **10**^{Ext}. For **10**^{Cont}, we postulate that the presence of the macrocycle around the triazolium unit hinders the Upy moieties and prevents an efficient stacking of the Upy-Upy dimers on top of each other. Indeed, a 45° shift between the two planes is required for an efficient formation of stacks,[42] which might be difficult to reach for the contracted form of the rotaxane. The hindrance of the macrocycle at the vicinity of the hydrogen-bonding pattern might also explain the relatively low dimerization constant of the Upy unit measured for **10**^{Cont} by ITC. Our explanation involving steric hindrance is also supported by recent literature on the molecular modelling of similar [c2]daisy chain rotaxanes revealing the partially folded conformation of the polymer when the macrocycles binds the triazolium in the contracted form.[43]

To further support our assumptions, we investigated the local configuration of **10**^{Cont} and **10**$^{Ext-G}$, as well as their global structures, by a combination of small-angle X-ray (SAXS) and small angle neutron (SANS) scattering experiments. In particular, SANS is a powerful technique to investigate at the same time the local configuration and the shapes of objects in solution in the range of 1-300 nm. The scattering curves normalized by the concentration for the two systems are depicted in Figure 4B,C.

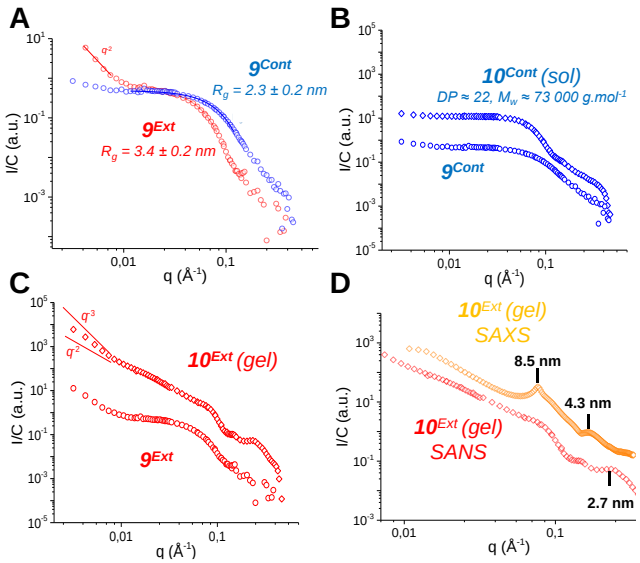

Figure 4. SANS curves for: (**A**) **9**^{Ext} and **9**^{Cont}; (**B**) **9**^{Cont} and **10**^{Cont}; (**C**) **9**^{Ext} and **10**^{Ext}, and (**D**) comparison of SANS and SAXS curves for **10**^{Ext} gel.

The two curves present different features: 1) in the low *q* regime, the normalized scattered intensity for **10**^{Cont} is completely flat, while the one for **10**$^{Ext-G}$ can be described

by a power law with an exponent close to -3 indicating the presence of large assemblies; 2) in the high q regime, fluctuations potentially corresponding to some ordering of the molecules composing the gel (structural peak) are observed for **10**^{Ext}, while the intensity related to **10**^{Cont} is rather smooth, indicating that there is no structural order within the contracted polymer; and 3) in the mid-q range, the **10**^{Cont} signal bends over reaching a plateau, while the **10**^{Ext} signal is still increasing. To understand the structural conformation of the two polymers, the corresponding monomers were measured (Figure 4A); which is of crucial importance for **10**^{Ext}. The monomer curves show the same overall behavior as the polymer ones, however there are two remarkable differences: 1) in the contracted state, the scattered intensity of **9**^{Cont} decays at a higher q value compared to **10**^{Cont}, indicating a difference between monomer and polymer dimensions; and 2) in the extended state, the scattered intensity for the monomer and the polymer decay at the same q value indicating that the cross-section remains unchanged. However, for polymer **10**^{Ext}, fluctuations of the intensity, which are not present for monomer **9**^{Ext}, are observed in the middle q range. As discussed above, these structural peaks are specific of the gel formed by the extended polymer. For both extended monomer and polymer, and in contrast with the contracted state, the signal rises up at low q. These observations correspond to two different phenomena: for polymer **10**^{Ext}, it relates to inhomogeneities in the gel due to cross-link rich regions, while for monomer **9**^{Ext} it is probably due to the partial solubility of the compound in toluene. The monomer curves were fitted accordingly to the Guinier approximation (see supporting information section 3), providing Guinier radii R_g = 2.3 ± 0.2 nm for **9**^{Cont}, and R_g = 3.4 ± 0.2 nm for **9**^{Ext}. The Guinier approximation could not be used to fit the data for **10**^{Cont}, hence suggesting that the plateau is not strictly related to the finite size of the polymer, but rather to some structural ordering. However, the plateau at low q and, in particular, the intensity at q = 0 of the contracted monomer and polymer curve provides information on the degree of polymerization. In this case, the contracted polymer **10**^{Cont} is composed of 22 monomers. This result is in perfect agreement with the association constant measured by ITC. At this concentration, and assuming that the polymerization occurs *via* an isodesmic mechanism,[44] the expected degree of polymerization should be $n = [C.K_a]^{1/2} = [4.32 \times 10^{-2} \times 1.1 \times 10^4]^{1/2} \approx 22$. For the extended polymer **10**^{Ext}, the scattering pattern is rather complex and no Guinier regions are observed. To understand the structure of the gel, the SANS and SAXS curves were compared as shown in Figure 4D. The two curves present structural peaks at high q that correspond to three different characteristic lengths: d_1 = 8.5 nm, d_2 = 4.3 nm and d_3 = 2.7 nm. They provide information on the structural organization of the gel in the extended state. The first peak (8.5 nm) corresponds to the inter-reticulating distance while the second peak (4.3 nm) might be the second order fluctuation of the first. The peak at d_3 = 2.7 nm is related to the structure of the reticulation units. As already outlined, the monomers are connected by hydrogen bonding but can also stack by π-π interactions. Moreover, the stacking takes place with a 45° shift between the two planes, leading to the formation of a helical structure. The characteristic length d_3 = 2.7 can be associated to the size of the helical pitch, or to the average size of these stacks. In addition, neglecting the upturn due to inhomogenieties at very low q, **10**^{Ext} SANS curve shows a contribution at low q corresponding to a finite size of around 20 nm, which may be related to the mesh size of the network. To summarize, the extended polymer **10**^{Ext} forms a network with a mesh size of 20 nm, helical reticulating nodes due to π-π stacking of the Upy dimers associated with the peak at 2.7 nm and an inter-reticulating nodes distance of 8.5 nm. This is very different from the contracted polymer **10**^{Cont} that only consists in a single chain of 22 monomers. For **10**^{Cont}, SAXS confirms the plateau at low q and the smooth decay at high q (Figure S12).

Overall, these experiments confirm that lateral ordering of the polymer chain occurs in **10**^{Ext}, while such organization is not present in **10**^{Cont}, because of the proximity of the macrocycle with the Upy dimers, thus destabilizing the hydrogen bonding association and preventing lateral π- π stacking interactions (Figure 5).

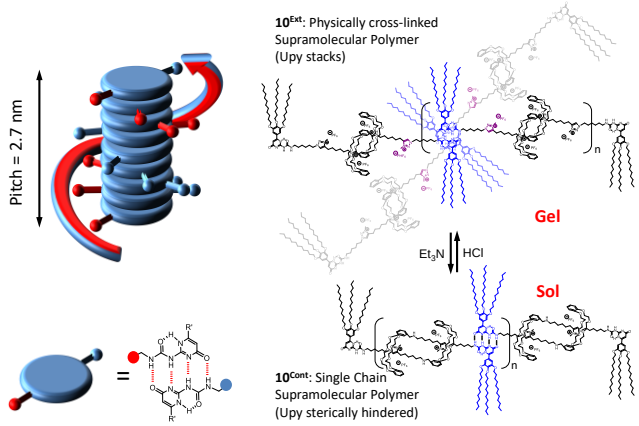

Figure 5. Overview of the nano-mechanically activated sol-gel transition by destabilization of the Upy stacks in the contracted supramolecular polymer.

Conclusion

We have described the synthesis of Upy-functionalized bistable [c2]daisy chains rotaxanes and their subsequent polymerization in both contracted and extended forms. In aromatic apolar solvents such as toluene and at the studied concentration, **10**^{Ext} forms a gel while **10**^{Cont} remains as a solution. The sol-gel transition can be controlled *in situ* by actuation of the bistable [c2]daisy chains, which in turn changes the association properties of the supramolecular polymers at the same concentration. The change of the physical state is attributed locally to the steric hindrance of the crown ether which, in the contracted form, comes in the vicinity of the Upy groups and prevents the

formation of lateral stacks of Upy-Upy dimers. Thus, the macroscopic physical state of the material is governed by the position of the mechanical bond at nanoscale. This shines light on how future architectures should be designed to avoid or include such (de)stabilizing effects. This original example of a reversible sol-gel transition induced by a nano-mechanical actuation illustrates one of the very interesting possibilities offered by the implementation of molecular machines in new kinds of responsive materials.

ASSOCIATED CONTENT

Supporting Information. Synthetic protocols and characterization of compounds **1–9**, synthetic protocols for the photo-deprotection of UPy rotaxanes, additional characterizations of the corresponding polymers, SANS and SAXS experimental procedures. This material is available free of charge via the Internet at http://pubs.acs.org.

AUTHOR INFORMATION

Corresponding Author

giuseppone@unistra.fr

ACKNOWLEDGMENTS

This work was supported by the Agence Nationale pour la Recherche (Grant number ANR-14-CE06-0021, fellowships to A.G., T.L. and G.M.) and the French Ministry of Research (fellowship to A.G.). We wish to thank the Laboratory of Excellence for Complex System Chemistry (LabEx CSC), the international center for Frontier Research in Chemistry (icFRC), the Centre National de la Recherche Scientifique (CNRS), the COST action (CM 1304), the University of Strasbourg (UdS), the University of Paris Diderot (Sorbonne Paris Cité) and the Institut Universitaire de France (N.G.) for financial supports. We also wish to thank the Laboratoire Léon Brilloin (LLB, CEA, Saclay, France) for beamtime allocation, Dr. Jean-Marc Strub for HRMS experiments and Dr. Mélanie Legros and Cathy Saettel for TGA and DSC experiments.

ABBREVIATIONS

2-Ureido-4[1H]-pyrimidinone, Upy; *tert*-butyldiphenylsilyl chloride, TBDPSCl; dimethylformamide, DMF; tetrabutylammonium fluoride, TBAF; tetrahydrofuran, THF; High Resolution Mass Spectrometry HRMS.

REFERENCES

(1) Abendroth, J. M.; Bushuyev, O. S.; Weiss, P. S.; Barrett, C. J. *ACS Nano* **2015**, *9*, 7746.

(2) Erbas-Cakmak, S.; Leigh, D. A.; McTernan, C. T.; Nussbaumer, A. L. *Chem. Rev.* **2015**, *115*, 10081.

(3) Coskun, A.; Banaszak, M.; Astumian, R. D.; Stoddart, J. F.; Grzybowski, B. A. *Chem. Soc. Rev.* **2012**, *41*, 19.

(4) Browne, W. R.; Feringa, B. L. *Nat. Nanotechnol.* **2006**, *1*, 25.

(5) Schliwa, M.; Woehlke, G. *Nature* **2003**, *422*, 759.

(6) Kinbara, K.; Aida, T. *Chem. Rev.* **2005**, *105*, 1377.

(7) Krans, J. L. *Nat. Educ.* **2010**, *3*, 66.

(8) Iwaso, K.; Takashima, Y.; Harada, A. *Nat. Chem.* **2016**, *8*, 625.

(9) Berna, J.; Leigh, D. A.; Lubomska, M.; Mendoza, S. M.; Perez, E. M.; Rudolf, P.; Teobaldi, G.; Zerbetto, F. *Nat Mater* **2005**, *4*, 704.

(10) Iamsaard, S.; Aßhoff, S. J.; Matt, B.; Kudernac, T.; Cornelissen, J. J. L. M.; Fletcher, S. P.; Katsonis, N. *Nat. Chem.* **2014**, *6*, 229.

(11) Li, Q.; Fuks, G.; Moulin, E.; Maaloum, M.; Rawiso, M.; Kulic, I.; Foy, J. T.; Giuseppone, N. *Nat. Nanotechnol.* **2015**, *10*, 161.

(12) Eelkema, R.; Pollard, M. M.; Vicario, J.; Katsonis, N.; Ramon, B. S.; Bastiaansen, C. W. M.; Broer, D. J.; Feringa, B. L. *Nature* **2006**, *440*, 163.

(13) Foy, J.; Li, Q.; Goujon, A.; Colard-Itté, J.-R.; Fuks, G.; Moulin, E.; Schiffmann, O.; Dattler, D.; Funeriu, D.; Giuseppone, N. *Nat. Nanotechnol.* **2017**, *12*, DOI: 10.1038/nnano.2017.28.

(14) Wolf, A.; Moulin, E.; Cid Martín, J. J.; Goujon, A.; Du, G.; Busseron, E.; Fuks, G.; Giuseppone, N. *Chem. Commun.* **2015**, *51*, 4212.

(15) Zhang, Z.; Han, C.; Yu, G.; Huang, F. *Chem. Sci.* **2012**, *3*, 3026.

(16) Jiménez, M. C.; Dietrich-Buchecker, C.; Sauvage, J.-P. *Angew. Chem. Int. Ed.* **2000**, *39*, 3284.

(17) Fang, L.; Hmadeh, M.; Wu, J.; Olson, M. A.; Spruell, J. M.; Trabolsi, A.; Yang, Y. W.; Elhabiri, M.; Albrecht-Gary, A. M.; Stoddart, J. F. *J. Am. Chem. Soc.* **2009**, *131*, 7126.

(18) Clark, P. G.; Day, M. W.; Grubbs, R. H. *J. Am. Chem. Soc.* **2009**, *131*, 13631.

(19) Du, G.; Moulin, E.; Jouault, N.; Buhler, E.; Giuseppone, N. *Angew. Chem. Int. Ed.* **2012**, *51*, 12504.

(20) Goujon, A.; Du, G.; Moulin, E.; Fuks, G.; Maaloum, M.; Buhler, E.; Giuseppone, N. *Angew. Chem. Int. Ed.* **2016**, *55*, 703.

(21) Gao, L.; Zhang, Z.; Zheng, B.; Huang, F. *Polym. Chem.* **2014**, *5*, 5734.

(22) Shimizu, L. S. *Polym. Int.* **2007**, *56*, 444.

(23) González-Rodríguez, D.; Schenning, A. P. H. J. *Chem. Mater.* **2011**, *23*, 310.

(24) Beijer, F. H.; Sijbesma, R. P.; Kooijman, H.; Spek, A. L.; Meijer, E. W. *J. Am. Chem. Soc.* **1998**, *120*, 6761.

(25) Söntjens, S. H. M.; Sijbesma, R. P.; van Genderen, M. H. P.; Meijer, E. W. *J. Am. Chem. Soc.* **2000**, *122*, 7487.

(26) Yang, Y.; Xue, M.; Marshall, L. J.; De Mendoza, J. *Org. Lett.* **2011**, *13*, 3186.

(27) Sijbesma, R. P.; Beijer, F. H.; Brunsveld, L.; Folmer, B. J.; Hirschberg, J. H.; Lange, R. F.; Lowe, J. K.; Meijer, E. W. *Science* **1997**, *278*, 1601.

(28) Bosman, A. W.; Sijbesma, R. P.; Meijer, E. W. *Mater. Today* **2004**, *7*, 34.

(29) Kautz, H.; van Beek, D. J. M.; Sijbesma, R. P.; Meijer, E. W. *Macromolecules* **2006**, *39*, 4265.

(30) Wei, P.; Yan, X.; Cook, T. R.; Ji, X.; Stang, P. J.; Huang, F. *ACS Macro Lett.* **2016**, *5*, 671.

(31) Fu, X.; Gu, R.-R.; Zhang, Q.; Rao, S.-J.; Zheng, X.-L.; Qu, D.-H.; Tian, H. *Polym. Chem.* **2016**, *7*, 2166.

(32) Hirschberg, J. H. K. K.; Koevoets, R. A.; Sijbesma, R. P.; Meijer, E. W. *Chem. Eur. J.* **2003**, *9*, 4222.

(33) Hosono, N.; Gillissen, M. A. J.; Li, Y.; Sheiko, S. S.; Palmans, A. R. A.; Meijer, E. W. *J. Am. Chem. Soc.* **2013**, *135*, 501.

(34) Romuald, C.; Busseron, E.; Coutrot, F. *Org. Lett.* **2008**, *10*, 3741.

(35) Van Beek, D. J. M.; Spiering, A. J. H.; Peters, G. W. M.; Te Nijenhuis, K.; Sijbesma, R. P. *Macromolecules* **2007**, *40*, 8464.

(36) Armstrong, G.; Buggy, M. *Mater. Sci. Eng. C* **2001**, *18*, 45.

(37) Arnaud, A.; Bouteiller, L. *Langmuir* **2004**, *20*, 6858.

(38) Brunsveld, L.; Vekemans, J. A. J. M.; Hirschberg, J. H. K. K.; Sijbesma, R. P.; Meijer, E. W. *Proc. Natl. Acad. Sci.* **2002**, *99*, 4977.

(39) Hirschberg, J. H. K. K.; Brunsveld, L.; Ramzi, A.; Vekemans, J. A. J. M.; Sijbesma, R. P.; Meijer, E. W. *Nature* **2000**, *407*, 167.
(40) Cyrański, M. K.; Gilski, M.; Jaskólski, M.; Krygowski, T. M. *J. Org. Chem.* **2003**, *68*, 8607.
(41) Botterhuis, N. E.; van Beek, D. J. M.; van Gemert, G. M. L.; Bosman, A. W.; Sijbesma, R. P. *J. Polym. Sci. Part A Polym. Chem.* **2008**, *46*, 3877.
(42) Guo, D.; Sijbesma, R. P.; Zuilhof, H. *Org. Lett.* **2004**, *6*, 3667.
(43) Zhao, Y.-L.; Zhang, R.-Q.; Minot, C.; Hermann, K.; Van Hove, M. A. *Phys. Chem. Chem. Phys.* **2015**, *17*, 18318.
(44) De Greef, T. F. A.; Smulders, M. M. J.; Wolffs, M.; Schenning, A. P. H. J.; Sijbesma, R. P.; Meijer, E. W. *Chem. Rev.* **2009**, *109*, 5687.

Graphical Abstract